PERGAMON

International Journal of Solids and Structures 37 (2000) 2507–2518

INTERNATIONAL JOURNAL OF SOLIDS and STRUCTURES

www.elsevier.com/locate/ijsolstr

Elastica and buckling load of simple tapered columns with constant volume

B.K. Lee[a,*], S.J. Oh[b,1]

[a]*Department of Civil Engineering, Wonkwang University, Iksan, Junbuk 570-749, South Korea*
[b]*Engineering Research Institute, Wonkwang University, Iksan, Junbuk 570-749, South Korea*

Received 26 February 1998

Abstract

Numerical methods are developed for solving the elastica and the buckling load of simply supported tapered columns subjected to compressive end load. The linear, parabolic and sinusoidal tapers with the regular polygon cross-sectional shapes are considered, whose material volumes are always held constant. The column model is based on Bernoulli–Euler beam theory. The Runge–Kutta and Regula–Falsi methods are used to solve the buckling load and the postbuckling deflected shape vs load. Extensive numerical results, including the equilibrium paths, the shapes of elastica and the buckling loads are presented in non-dimensional forms. By varying the section ratio, the strongest columns are identified for each taper and cross-sectional shape.

Keywords: Elastica; Buckling load; Tapered column; Constant volume; Strongest column

1. Introduction

The first studies of the elastica were published by Euler (1774). A survey of the classical literature on this subject was published by Schmidt and Da Deppo (1971). Present-day applications of elastica including statics and dynamics problems were discussed by Wilson and Mahajan (1989) and Lee et al. (1993), respectively. Other works related to the present studies, especially those involving uniform beams, were studied by Love (1927), Timoshenko and Gere (1961), Rojahn (1968), Wang (1981), Wilson and Snyder (1988), Lee (1990), Chucheepsakul et al. (1995), and Chucheepsakul et al. (1996).

* Corresponding author. Fax: +82-653-857-7204.
E-mail address: bkleest@wonnms.wonkwang.ac.kr (B.K. Lee)
[1] Present address: Department of Civil Engineering, Provincial College of Damyang, Chonnam 517-800, South Korea.

0020-7683/00/$ - see front matter
PII: S0020-7683(99)00007-4

Since columns are basic structural forms, these units have been widely used in various engineering fields. In column problems, both the buckling loads and postbuckling behavior are very important to structural design. The column behavior under loads depends on the cross-sectional shape, taper type and volume of the column (Gere and Timoshenko, 1984; Haftka et al., 1990). Especially estimating the buckling loads of nonprismatic columns, which have the same volume with specific length, are attractive in the viewpoint of optimal design. Since Lagrange (1773) attempted to determine the optimum shape for a column, many investigators including Clausen (1849), Keller (1960), Tadjbakhsh and Keller (1962), Barnes (1988), and Cox and Overton (1992) determined the shape of the strongest column which is defined as the elastic column of a given length and volume which can carry the highest axial load without buckling. In the most previous works related on the strongest column, only the equilateral triangular, square and circular were considered as the cross-section. Considering the erecting condition and the aesthetic viewpoint, the cross-sections of regular polygon are sometimes needed in the practical engineering fields. Nowhere in the open literature gave the solutions for the class of elastica problems considered herein; the elastica and buckling load of nonuniform or tapered columns of regular polygon cross-section with constant volume, whose cross-sectional depths are varied by functional fashions. The main purpose of this paper is to investigate both the buckling loads and elastica of such columns.

In the analysis of elastica, one usually begins with the classical Bernoulli–Euler beam theory, the nonlinear differential equation that relates deflection to load. This beam theory is also used in the present analytical studies. The following assumptions are inherent in this theory; the column is linearly elastic, the neutral axis for bending is incompressible, and transverse shear deformations are negligible.

Historically, solutions of elastica have four forms: (1) closed-form solutions in terms of elliptic integrals; (2) power series solutions; (3) numerical solutions; and (4) experimental solutions. The present study should be classified into the numerical solutions.

2. Object column

Shown in Fig. 1(a) is the object column of specific length l and of constant volume V. All the columns analyzed in this study have the same length and the same volume. Its cross-sectional shape is the regular polygon, whose cross-sectional depth depicted as h varies with the axial length s. The area and second moment of area of cross-section depicted as A and I, respectively, vary with s. Figure 1(b) shows the

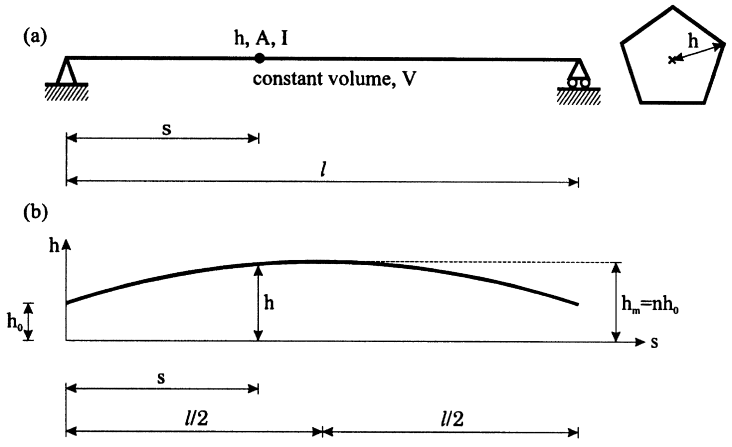

Fig. 1. Column with constant volume and its variation of cross-sectional depth.

variation of depth h with s. As shown in this figure, the depth h is varied by functional fashion, and depths h at $s = 0$ and l, and at $s = l/2$ are h_0 and h_m, respectively. For defining geometry of column, a non-dimensional system parameter or section ratio n is introduced as follows.

$$n = h_m/h_0 \tag{1}$$

The area A and second moment of area I of the regular polygon cross-section with integer m of side number and cross-sectional depth h are given by, respectively,

$$A = c_1 h^2 \tag{2}$$

$$I = c_2 h^4 \tag{3}$$

where

$$c_1 = m \sin(\pi/m) \cos(\pi/m) \tag{4.1}$$

$$c_2 = m \sin(\pi/m) \cos^3(\pi/m)\left[1 + \tan^2(\pi/m)/3\right]/4 \tag{4.2}$$

in which the values of c_1 and c_2 with infinite number $m(\infty)$, namely circular cross-section, are converged to π and $\pi/4$, respectively. Also, it is noted that every axis across the centroid of a regular polygon cross-section is a principal axis and has the same second moment of area given in eqn (3).

Now, consider the functional equations of variable depth h. It is natural that all columns whose variable depth are prescribed should be the object ones. In this study, the linear, parabolic and sinusoidal tapers are chosen as the variable depth h of tapered columns. First, the equation h of linear taper through three points of $(0, h_0)$, $(l/2, nh_0)$ and (l, h_0) in rectangular co-ordinates (s, h) are obtained as follows.

$$h = h_0\left[2c_3(s/l) + 1\right], \quad 0 \leqslant s \leqslant l/2$$

$$h = h_0\left[-2c_3(s/l) + 2c_3 + 1\right], \quad l/2 \leqslant s \leqslant l \tag{5}$$

where

$$c_3 = n - 1 \tag{6}$$

The column's volume V can now be calculated by using eqns (2) and (5):

$$V = \int_0^l A \, \mathrm{d}s$$

$$= c_4\left(c_1 h_0^2 l\right) \tag{7}$$

where

$$c_4 = V/\left(c_1 h_0^2 l\right)$$

$$= \left(n^2 + n + 1\right)/3 \tag{8}$$

In the above equation, c_4 is defined as a ratio of constant volume V to volume of uniform column of regular polygon cross-section with depth h_0, $c_1 h_0^2 l$.

Second, the equation h and c_4 value of parabolic taper are given by

$$h = h_0\left[-4c_3(s/l)^2 + 4c_3(s/l) + 1\right], \quad 0 \leqslant s \leqslant l \tag{9}$$

$$c_4 = \left(8n^2 + 4n + 3\right)/15 \tag{10}$$

Finally, the equation h and c_4 value of sinusoidal taper are, respectively,

$$h = h_0\left[c_3 \sin(\pi s/l) + 1\right], \quad 0 \leqslant s \leqslant l \tag{11}$$

$$c_4 = (n-1)^2/2 + 4(n-1)/\pi + 1 \tag{12}$$

In eqns (9) and (11), c_3 is defined in eqn (6).

3. Mathematical model

The symbols and loading for the column defined in above section are depicted in Fig. 2. The column is supported by the hinged and movable ends. The column subjected to a compressive end load P less than the buckling load B is perfectly straight. But when the P exceeds the B, the column is buckled. The dashed line and the solid curve are the neutral axes of the unbuckled and buckled column, respectively. Thus the shape of elastica is the solid curve defined by the (x, y) co-ordinate system whose origin is at hinged end. At material point (x, y), the column's arc length is s, and the variable area and second moment of area of cross-section taken with respect to s are A and I, respectively. The rotation of cross-section and bending moment are depicted as θ and M, respectively, in this figure. The axis length of buckled column maintains its length l due to incompressibility of column, and therefore the s value at movable end is l. The rotation at hinged end ($s = 0$) and the horizontal displacement at movable end ($s = l$) are α and Δ, respectively. It is assumed that the Bernoulli–Euler theory governs the buckled column behavior under load, for which the differential equations of the elastica (Timoshenko and Gere, 1961) are

$$\mathrm{d}\theta/\mathrm{d}s = -Py/EI, \quad 0 \leqslant s \leqslant l \tag{13}$$

$$\mathrm{d}x/\mathrm{d}s = \cos\theta, \quad 0 \leqslant s \leqslant l \tag{14}$$

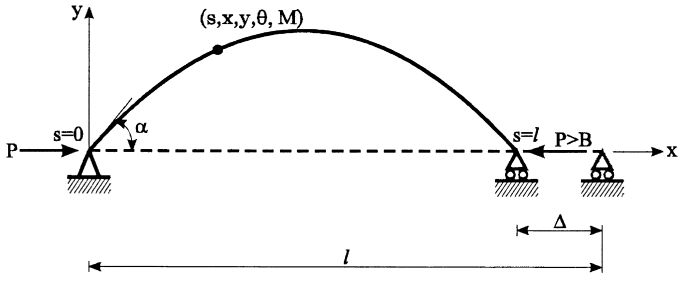

Fig. 2. Variables of elastica of buckled column.

$$dy/ds = \sin\theta, \quad 0 \leqslant s \leqslant l \tag{15}$$

where E is Young's modulus and the term of Py in eqn (13) is the bending moment M at the material point (x, y).

Since the horizontal and vertical displacements at hinged ends ($s = 0$) are not allowed, the following boundary conditions are obtained:

$$x = 0 \quad \text{at} \quad s = 0 \tag{16}$$

$$y = 0 \quad \text{at} \quad s = 0 \tag{17}$$

Since the vertical displacement at movable end ($s = l$) is not allowed, the boundary condition is

$$y = 0 \quad \text{at} \quad s = l \tag{18}$$

To facilitate the numerical studies and to obtain the most general results for this class of problem, the axial load, the geometric parameters, and the governing differential equations with their boundary conditions are cast in the following non-dimensional forms. The first is the load parameter,

$$p = Pl^2/(\pi^2 EI_e) \tag{19}$$

where I_e is the second moment of area of circular cross-section of uniform column whose volume is V, defined as

$$I_e = V^2/(4\pi l^2) \tag{20}$$

In the above two equations, the load parameter p is defined by using the constant volume V and the specific length l in order to compare all the responses of columns regardless of taper type, side number m and section ratio n.

The arc length s and coordinates (x, y) are normalized by the column length l, or

$$\lambda = s/l \tag{21}$$

$$\xi = x/l \tag{22}$$

$$\eta = y/l \tag{23}$$

The displacement Δ of movable end ($s = l$) is also normalized by l, or

$$\delta = \Delta/l \tag{24}$$

When eqn (3) is combined with either eqn (5) or eqn (9) or eqn (11), and eqns (19)–(23) are used, the non-dimensional form of eqn (13) becomes

$$d\theta/d\lambda = -\pi c_1^2 c_4^2 p\eta/(4c_2 i), \quad 0 \leqslant \lambda \leqslant 1 \tag{25.1}$$

where for linear taper:

$$i = (2c_3\lambda + 1)^4, \quad 0 \leqslant \lambda \leqslant 0.5$$

$$i = (-2c_3\lambda + 2c_3 + 1)^4, \quad 0.5 \leqslant \lambda \leqslant 1 \tag{25.2}$$

for parabolic taper:

$$i = \left(-4c_3\lambda^2 + 4c_3\lambda + 1\right)^4, \quad 0 \leqslant \lambda \leqslant 1 \tag{25.3}$$

for sinusoidal taper:

$$i = \left[c_3 \sin(\pi\lambda) + 1\right]^4, \quad 0 \leqslant \lambda \leqslant 1 \tag{25.4}$$

It is recalled that the coefficients c_1–c_4 of differential eqn (25.1) with eqns (25.2)–(25.4) contain the side number m and section ratio n, respectively, as shown in the previous section.

Further, with eqns (21)–(23), eqns (14) and (15) become

$$\mathrm{d}\xi/\mathrm{d}\lambda = \cos\theta, \quad 0 \leqslant \lambda \leqslant 1 \tag{26}$$

$$\mathrm{d}\eta/\mathrm{d}\lambda = \sin\theta, \quad 0 \leqslant \lambda \leqslant 1 \tag{27}$$

The non-dimensional forms for boundary conditions of eqns (16)–(18) are obtained by eqns (21)–(23):

$$\xi = 0 \quad \text{at} \quad \lambda = 0 \tag{28}$$

$$\eta = 0 \quad \text{at} \quad \lambda = 0 \tag{29}$$

$$\eta = 0 \quad \text{at} \quad \lambda = 1 \tag{30}$$

For other end constraints e.g. clamped–clamped, clamped–movable, and clamped–free ends, the corresponding boundary conditions can be easily obtained by the similar process mentioned above.

4. Numerical methods

Based on the above analysis, the algorithm was developed to solve differential eqns (25.1), (26) and (27). The Runge–Kutta and Regula–Falsi methods (Carnahan et al., 1969) were used to integrate differential equations and to determine the rotation of the cross-section at $\lambda = 0$, α, for a given geometry of column. This algorithm is summarized as follows:

(1) specify taper type (linear/parabolic/sinusoidal), geometry (m and n), and load p. Calculate c_1-c_4. It is recalled that m is the integer number of sides of regular polygon cross-section;
(2) assume a trial value α_t in which first trial value is zero;
(3) integrate eqns (25.1), (26) and (27) with the boundary conditions of eqns (28) and (29) in the range from $\lambda = 0$ to 1 using the Runge–Kutta method. The results give trial solutions for $\theta = \theta(\lambda)$, $\xi = \xi(\lambda)$ and $\eta = \eta(\lambda)$.
(4) set $D = \eta(1)$. If the value of α_t assumed in step 2 is the characteristic value of the elastica, then D must be zero due to eqn (30). The first criterion for convergence of the solutions is $|D| \leqslant 1 \times 10^{-10}$;
(5) if the value of D does not satisfy the first convergence criterion, then increment the previous value of α_t;
(6) repeat steps (3)–(5) and note the sign of D in each iteration. If D changes sign between two consecutive values α_1 and α_2 of α_t, then the characteristic value α lies between α_1 and α_2;
(7) compute an improved value of α_t based on its two previous values using the Regula–Falsi method. The second criterion for convergence of solutions is $|(\alpha_2 - \alpha_1)/\alpha_2| \leqslant 1 \times 10^{-5}$;

(8) terminate the calculations when two convergence criteria are met. Print the final solutions to the elastica, $\theta = \theta(\lambda)$, $\xi = \xi(\lambda)$ and $\eta = \eta(\lambda)$, and then compute the displacement $\delta = 1 - \xi(1)$. If there is no solution, which means that D does not change sign until the trial value of α_t reaches π, the specified p is less than b and the column is still straight. Here, b is the buckling load parameter defined as

$$b = Bl^2/(\pi^2 EI_e) \tag{31}$$

Also, the buckling load parameters b were calculated in a straightforward way using the differential equations. Just after the column is buckled, all values of column behavior including α are close to zero. In this study, the buckling load parameter b is approximately equivalent to the load parameter p whose rotation of cross section at $\lambda = 0$, α, is 1×10^{-10}, i.e. nearly zero but not zero. Specify column taper, m, n, of course not p and set $\theta = 1 \times 10^{-10}$ at $\lambda = 0$ in eqns (26) and (27). And assume the trial value p instead of α_t in step 2. Remaining numerical procedures are the same as the above procedure, and of course the characteristic value of eqn (25.1) is p which is now an approximate buckling load parameter b.

Based on these algorithms, two FORTRAN computer programs were written to solve the elastica and buckling loads, respectively. All computations were carried on a notebook computer with graphics support. For all of the numerical results presented herein, a step size of $\Delta\lambda = 1/50$ in the Runge–Kutta method was found to give convergence for α and b to within three significant figures. The numerical results are now discussed in the next section.

5. Numerical results and discussion

Firstly, we consider the elastica problem. Shown in Fig. 3 are the equilibrium paths of linear taper with $m = 3$, 4 and c (circular cross-section) for $n = 1.5$, which represents the deflections (α/π, δ and η_m) vs p curves after buckling. Here, η_m is defined as value of η at column's mid-point ($\lambda = 0.5$). The nonlinear responses of α/π and δ increase as p increases; those of η_m reach peaks as p is increased. The increasing rates of all responses are higher in lower p. Especially the rates are very high just after the

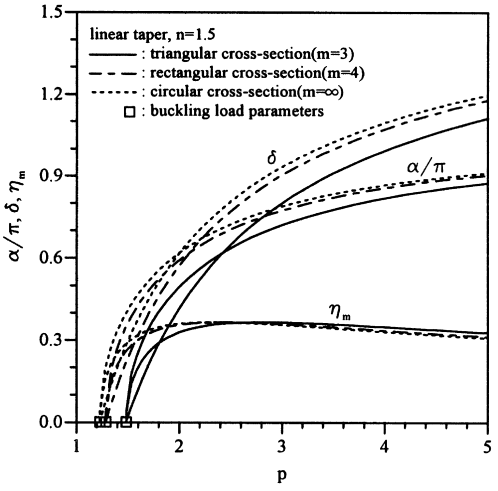

Fig. 3. Equilibrium path of linear taper with $n = 1.5$ by side number m.

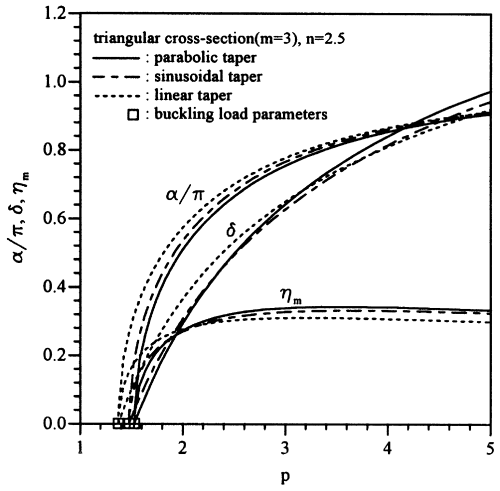

Fig. 4. Equilibrium path of columns with $m = 3$ and $n = 2.5$ by taper type.

columns are buckled. Just after buckling of the column, as the integer number m increases from $m = 3$ to $m = 4$ to $m = c(\infty)$, all deflections increase, other parameters remaining constant. But it is true that in the case of response η_m, the fact is reversed when p exceeds some characteristic value. It is seen that the p values marked by □ are the buckling load parameters b of corresponding columns. For example, the b of $m = 3$ is 1.484.

Shown in Fig. 4 are the equilibrium paths of parabolic, sinusoidal and linear tapers for $m = 3$ and $n = 2.5$. Just after buckling, as the taper type is changed from parabolic to sinusoidal to linear taper, the response of α/π increases corresponding to this change, other parameters remaining constant. Also, the buckling load parameters are marked by □ on the p axis.

Figure 5 shows the elastica of linear taper with $m = 3$, 4, 5 and c for $n = 1.5$ and $p = 1.8$. From this Figure, as the m value increases from 3 to c, the horizontal and vertical deflections increase.

Secondly, we consider the buckling load problem. For the purpose of validation of this study, the buckling load parameters b and one buckling load B predicted by the present theory, respectively, are compared to those available in references in Table 1 which shows the results of this study quite agree with the reference values.

Shown in Figs. 6, 7, 8 are the b vs n curves of columns with $m = 3$, 4, 5 and c for linear, parabolic and sinusoidal taper, respectively. Each curve reaches a peak which is marked □. At these peak points, the columns corresponding to the given taper types show the largest b values which are the buckling load parameters of the strongest columns. Here the word 'strongest' used to mean 'most' resistant to

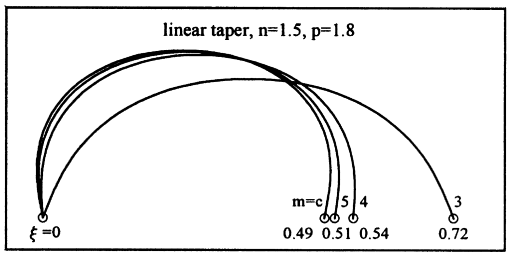

Fig. 5. Elastica of linear taper with $n = 1.5$ and $p = 1.8$ by side number m.

Table 1
Comparisons of b and B between this study and references

Geometry	b or B	
	This study	Reference
$n = 1$[a], $m = c$	$b = 1.0$	1.0 of ref. [A][c]
$n = 2.32$[b], $m = c$ Sinusoidal	$B = 553$ lbs (2460 N)	550 lbs of ref. [B][c] (2447 N)
$n = 1.98$, $m = 3$	$b = 1.574$	1.573 of ref. [C][c]
$n = 1.98$, $m = 4$	$b = 1.362$	1.363 of ref. [C][c]
$n = 1.98$, $m = 5$	$b = 1.323$	1.323 of ref. [C][c]
$n = 1.98$, $m = c$ Parabolic	$b = 1.301$	1.301 of ref. [C][c]

[a] If $n = 1$, the columns are uniform regardless of taper types. See eqns (25.2)–(25.4).
[b] $V = 9\pi/16$ in^3 (2.896×10^{-5} m^3), $l = 15.44$ in (0.3922 m), $E = 10 \times 10^6$ psi (6.895×10^{10} Pa).
[c] [A]: (Timoshenko and Gere, 1961) [B]: (Wilson et al., 1971) [C]: (Lee and Oh).

buckle. It is found that all the strongest columns occur at the same value n regardless of side number m if the taper type is same. And all b values of strongest columns decrease, as the m value is increased from 3 to c. The values of b and n of all strongest columns are summarized in Table 2. All b values of strongest columns are largest at $m = 3$ (triangular cross-section) and smallest at $m = c$ (circular cross-section), and the ratios of $m = 3$, 4 and 5, respectively, to $m = c$ are the same regardless of taper types. For example, the ratios of $m = 3$ to $m = c$ are 1.210 for all taper types.

Shown in Fig. 9 are the b vs n curves of parabolic, sinusoidal and linear tapers, respectively, for $m = 3$, in which the strongest columns are marked by □. The strongest of all columns by taper type is the parabolic tapered column as shown in this Figure and Table 2. The effect of taper type on b is negligible when n is less than about 1.3.

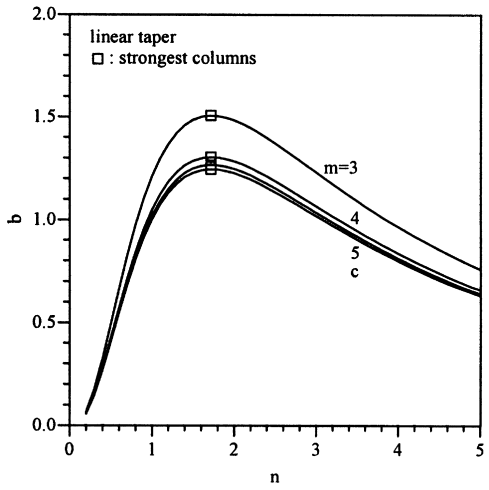

Fig. 6. b vs n curves of linear taper by side number m.

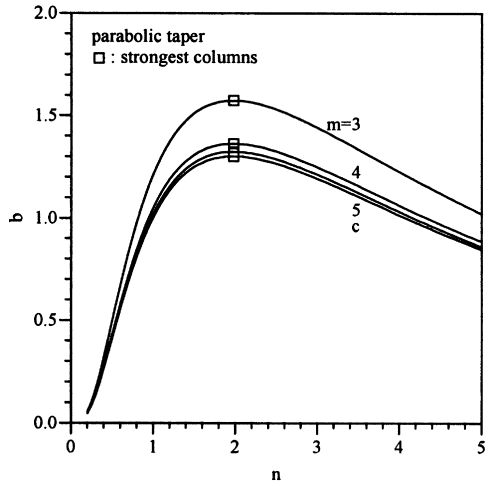

Fig. 7. b vs n curves of parabolic taper by side number m.

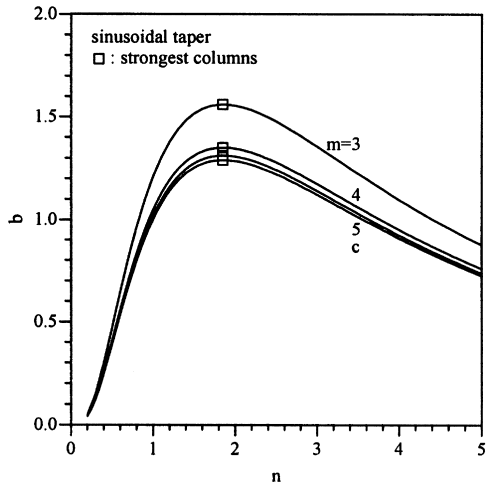

Fig. 8. b vs n curves of sinusoidal taper by side number m.

Shown in Fig. 10 are the elastica of strongest columns of $m = 3$ and $p = 2$ by taper type. The horizontal and vertical deflections increase, as the taper type is increased from parabolic to sinusoidal to linear taper, other parameters remaining constant.

6. Concluding remarks

The numerical methods developed herein for computing the elastica and buckling loads of simple tapered columns of regular polygon cross-section with constant volume were found to be efficient, and highly versatile. The differential equations governing the elastica of such column were derived and solved numerically. The linear, parabolic and sinusoidal tapers were chosen for the variable cross-sectional depth. As the numerical results, the equilibrium paths and elastica were presented, and the

Table 2
Values of n and b of the strongest columns by taper type and side number m

Taper type	m	n	b	Ratio[a]
Linear taper	3	1.72	1.505	1.210
	4	1.72	1.303	1.047
	5	1.72	1.265	1.017
	c	1.72	1.244	1.000
Parabolic taper	3	1.98	1.574	1.210
	4	1.98	1.362	1.047
	5	1.98	1.323	1.017
	c	1.98	1.301	1.000
Sinusoidal taper	3	1.85	1.559	1.210
	4	1.85	1.350	1.047
	5	1.85	1.311	1.017
	c	1.85	1.289	1.000

[a] Ratio of b of $m = 3$, 4 and 5, respectively, to $m = c$.

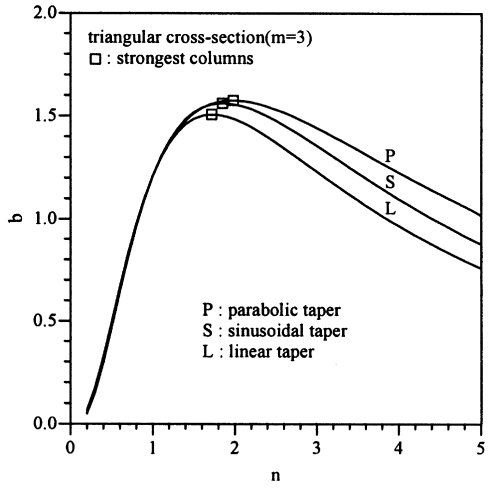

Fig. 9. b vs n curves by taper type.

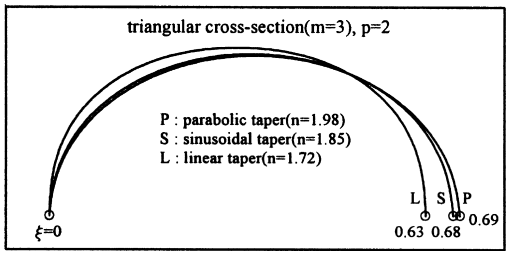

Fig. 10. Elastica of strongest columns with $m = 3$ and $p = 2$.

buckling load parameter vs section ratio (b vs n) curves were also reported. The strongest columns by taper type and side number of regular polygon cross section were determined by reading the peak point of buckling load parameters and their corresponding section ratios on b vs n curves.

In this paper, the column of hinged-movable end constraint not subjected to end moments is considered, and the column problem of other end constraints subjected to end moments will be presented in the near future.

Acknowledgement

This paper was supported by the Wonkwang University in 1997. The first author gives thanks for this financial support.

References

Barnes, D.C., 1988. The shape of the strongest column is arbitrarily close to the shape of the weakest column. Quarterly of Applied Mathematics 46, 605–609.

Carnahan, B., Luther, H.A., Wilkes, J.O., 1969. Applied Numerical Methods. Wiley, New York.

Chucheepsakul, S., Buncharon, S., Huang, T., 1995. Elastica of simple variable-arc-length beams subjected to end moment. Journal of Engineering Mechanics (ASCE) 121, 722–767.

Chucheepsakul, S., Thepphitak, G., Wang, C.M., 1996. Large deflection of simple variable-arc-length beams subjected to a point load. Structural Engineering and Mechanics 4, 49–59.

Clausen, T., 1849–1853. Uber lie Form architektonischer Saulen. Bulletin physico-Mathematiques et Astronumiques, 279–294. Summarized in Todhunter, I., Pearson, K., 1893. A History of the Theory of Elasticity and of the Strength of Materials, Cambridge Press.

Cox, S.J., Overton, M.I., 1992. On the optimal design of columns against buckling. SIAM Journal on Mathematical Analysis 23, 287–325.

Euler, L., 1774. Methodus Inveniendi Lineas Curvas Maxima Minimive Proprietate Gaudentes, Additamentum I. De Curvis Elasticis, Lausanne and Geneva.

Gere, J.M., Timoshenko, S.P., 1984. Mechanics of Materials, Brooks/Cole Engineering Division.

Haftka, R.T., Gurdal, Z., Kamat, M.P., 1990. Elements of Structural Optimization, Kluwer Academic Publishers, Dardrecht.

Keller, J.B., 1960. The shape of the strongest column. Archive for Rational Mechanics and Analysis 5, 275–285.

Lagrange, J.L., 1770–1773. Sur la Figure des Colonnes. Miscellanea Taurinesia 5, 123. Summarized in Todhunter, I., Pearson, K., 1886. A History of the Theory of Elasticity and of the Strength of Materials, Cambridge Press.

Lee, B.K., 1990. Numerical analysis of large deflections of cantilever beams. Journal of Korean Society of Civil Engineers 10, 1–7.

Lee, B.K., Oh, S.J., Free vibrations and buckling loads of tapered columns of regular polygon cross-section with constant volume. International Journal for Numerical Methods in Engineering (in review at present time).

Lee, B.K., Wilson, J.F., Oh, S.J., 1993. Elastica of cantilevered beams with variable cross-section. International Journal of Non-Linear Mechanics 28, 579–589.

Love, A.E.H., 1927. A Treatise on the Mathematical Theory of Elasticity. Dover.

Rojahn, C., 1968. Large deflections of elastic beam, Thesis for the Degree of Engineer, Stanford University.

Schmidt, R., Da Deppo, D.A., 1971. A survey of literature on large deflection of nonshallow arches, bibliography of finite deflections of straight and curved beams, rings, and shallow arches. The Journal of the Industrial Mathematics Society 21, 91–114.

Tadjbakhsh, I., Keller, J.B., 1962. Strongest columns and isoperimetric inequalities for eigenvalues. Journal of Applied Mechanics (ASME) 29, 159–164.

Timoshenko, S.P., Gere, J.M., 1961. Theory of Elastic Stability. McGraw-Hill, New York.

Wang, C.Y., 1981. Large deflections of an inclined cantilever with an end load. International Journal of Non-Linear Mechanics 16, 155–164.

Wilson, J.F., Holloway, D.M, Biggers, S.B., 1971. Stability experiments on the strongest columns and circular arches. Experimental Mechanics 11, 303–308.

Wilson, J.F., Mahajan, U., 1989. The mechanics and positioning of highly flexible manipulator limbs. Journal of Mechanism, Transmissions, and Automation Design III, 232–235.

Wilson, J.F., Snyder, J.M., 1988. The elastica with end-load flip-over. Journal of Applied Mechanics (ASME) 55, 845–848.